Microchimica Acta
https://doi.org/10.1007/s00604-017-2632-2

ORIGINAL PAPER

Fluorometric determination of nucleic acids based on the use of polydopamine nanotubes and target-induced strand displacement amplification

Jia Ge[1] · Dong-Mei Bai[1] · Xin -Geng[1] · Ya-Lei Hu[1] · Qi-Yong Cai[2] · Ke Xing[1] · Lin Zhang[1] · Zhao-Hui Li[1,2]

Received: 13 September 2017 / Accepted: 22 December 2017

Abstract

The authors describe a fluorometric method for the quantitation of nucleic acids by combining (a) cycled strand displacement amplification, (b) the unique features of the DNA probe SYBR Green, and (c) polydopamine nanotubes. SYBR Green undergoes strong fluorescence enhancement upon intercalation into double-stranded DNA (dsDNA). The polydopamine nanotubes selectively adsorb single-stranded DNA (ssDNA) and molecular beacons. In the absence of target DNA, the molecular beacon, primer and SYBR Green are adsorbed on the surface of polydopamine nanotubes. This results in quenching of the fluorescence of SYBR Green, typically measured at excitation/emission wavelengths of 488/518 nm. Upon addition of analyte (target DNA) and polymerase, the stem of the molecular beacon is opened so that it can bind to the primer. This triggers target strand displacement polymerization, during which dsDNA is synthesized. The hybridized target is then displaced due to the strand displacement activity of the polymerase. The displaced target hybridizes with another molecular beacon. This triggers the next round of polymerization. Consequently, a large amount of dsDNA is formed which is detected by addition of SYBR Green. Thus, sensitive and selective fluorometric detection is realized. The fluorescent sensing strategy shows very good analytical performances towards DNA detection, such as a wide linear range from 0.05 to 25 nM with a low limit of detection of 20 pM.

Keywords Biosensor · DNA detection · SYBR Green I · Molecular beacon · Klenow fragment

Introduction

The development of efficient fluorometric methods for ultrasensitive, rapid and cost-effective nucleic acids detection have attracted great attention since they play important roles in molecular diagnostics, identification of genetic mutations, monitoring of gene delivery, and biomedical development [1–4]. Methods such as fluorometry [5], electrochemistry [6], colorimetry [7], and surface-enhanced Raman spectroscopy (SERs) [8] have been developed for the detection of nucleic acids. Among these methods, owing to its simplicity, high sensitivity and homogeneity, fluorometry is one of the most widely used methods.

A variety of nanomaterials possess promising performance on detection of biomolecules [9–12]. Recently, a kind of biocompatible nanotubes has been broadly applied to biological areas, such as carbon nanotubes, silicon dioxide nanotubes, boron nitride nanotubes, titanium dioxide nanotubes, and organic nanotubes [13–16]. Among them, polydopamine nanotubes have attracted growing attention in the past decade because they combine good biocompatibility and unique electronic properties together, showing great potential as bioelectronic devices, biosensors, bioimaging agents and drug delivery in biomedical area, tissue engineering and photothermal therapy [17–21]. It has also been demonstrated that polydopamine

Electronic supplementary material The online version of this article (https://doi.org/10.1007/s00604-017-2632-2) contains supplementary material, which is available to authorized users.

✉ Jia Ge
jiage0630@hnu.edu.cn

✉ Zhao-Hui Li
zhaohui.li@zzu.edu.cn

[1] College of Chemistry and Molecular Engineering, Zhengzhou University, Zhengzhou 450001, People's Republic of China

[2] Institute of Chemical Biology and Nanomedicine, Hunan University, Changsha 410082, People's Republic of China

Published online: 10 January 2018

nanotubes exhibit a capability for discriminating single-stranded DNA (ssDNA) and double-stranded DNA (dsDNA), which may catalyze the applications of polydopamine nanotubes in biomedical areas [22]. To the best of our knowledge, the exploration of polydopamine nanotubes in biochemical application still remains at a very early stage. Moreover, it is still significant to acquire polydopamine nanotubes and explore its application as a universal biosensing platform.

Recently, various signal amplification strategies have been established for sensitive detection of DNA, such as hybridization chain reaction [23], exonuclease III assisted signal amplification [24], strand displacement amplification [25], rolling circle amplification [26] and catalytic hairpin assembly [27]. Among these signal amplification methods, the strand displacement amplification (SDA) is attracting much attention [28, 29]. The SDA uses a linear DNA sequence as template and repeatedly triggers the displacement polymerization reaction, in this case,the former products can be displaced by polymerases during the polymerization reaction, promoting the generation of the latter ones.

We present a novel fluorescence strategy based on strand displacement amplification for nucleic acids detection by using SYBR Green I (SG) as the signal readout and polydopamine nanotube as the adsorber. In the absence of the target DNA, the molecular beacon (MB), the primer and SG are adsorbed on polydopamine nanotubes, and the fluorescence of SG is quenched by polydopamine nanotubes following long range resonance energy transfer, resulting in a very low background signal. However, in the presence of the target DNA, MB is unfolded and the subsequent polymerization and strand displacement reaction take place to initiate the target recycling process. As a result, the strand displacement amplification for target DNA is achieved and large amount of dsDNA are formed. Upon the intercalation of SG into dsDNAs, a significantly enhanced fluorescence signal is generated due to the selective intercalation of SG into dsDNA detached from the polydopamine nanotubes surface. Thus sensitive fluorescence DNA assay based on strand displacement amplification on polydopamine nanotubes is realized.

Experimental procedures

Materials and apparatus

The oligonucleotides used were synthesized by Shanghai Sangon Biological Engineering Technology & Services Co., Ltd. (Shanghai, China, http://www.sangon.com/). The sequences of the DNA oligonucleotides were as follows:

Molecular beacon (MB): 5′ - TCT TGG ACA CAA ACT ATA CAA CCT ACT ACC TCA TGT GTC CAA GA-3′;
T 1 (target DNA): 5′ - TGA GGT AGT AGG TTG TAT AGTT-3′;
Primer 1: 5′- TCT TGG AC-3′;
Mismatched sequence 1 (M1):5′-TGA GGG AGT AGG TTG TAT AGTT -3′;
Mismatched sequence 1 (M2) :5′-TGA GCT AGT ACG TTG TAT AGTT -3′;
Mismatched sequence 1 (M3) :5′-TGA GCT AGT ACG TTG TCT AGTT-3′;
Random DNA: 5′-TGC AAG GTG TCA GTA TAA TCCG-3′

The Klenow fragment polymerase (KF polymerase, without 3' to 5' exonuclease activity) and deoxyribonucleoside triphosphates (dNTPs) were purchased from New England Biolabs (NEB, U. K., https://www.neb.com/). $ZnAc{\cdot}2H_2O$ was purchased from Aladdin (Shanghai, China). PEG 400 and Dopamine hydrochloride (99%) were purchased from Sigma-Aldrich Chemical Co. (St. Louis, MO, USA, https://www.sigmaaldrich.com/). SYBR Green I was purchased from Shanghai Sangon Biological Engineering Technology & Services Co., Ltd. (Shanghai, China, http://www.sangon.com/). All reagents were used as received without further purification. All solutions were prepared using ultrapure water, which was generated from a Millipore Milli-Q water purification system (Billerica, MA, USA) and had an electric resistance >18. 2 MΩ·cm.

The fluorescence measurements were carried out on a FL-4600 spectrophotometer (Hitachi, Japan). The fluorescence emission spectra were collected from 500 nm to 600 nm at room temperature with a 488 nm excitation wavelength.

Amplified DNA detection based on target strand-displacement polymerization reaction

100 μL of 10 mM Tris-HCl solution (50 mM NaCl, 10 mM $MgCl_2$, pH 7.4) containing 50 nM primer, 100 nM MB and different concentrations of target DNA were incubated at room temperature for 10 min. After which, 10 μL of KF polymerase (600 $U{\cdot}mL^{-1}$), 10 μL of dNTPs (200 μM) together with 20 μL of 10 × Klenow buffer (100 mM Tris–HCl, pH 7.5, 500 mM NaCl, 100 mM $MgCl_2$ and 10 mM dithiolthreitol) and 50 μL of ultrapure water were added and incubated at for 40 min at 37 °C. This step was followed by the addition of 5 μL polydopamine nanotubes (48 $\mu g{\cdot}mL^{-1}$) and 5 μL of 10 × SG solution. The final mixed solution with a total volume of 200 μL was kept in darkness at room

temperature for 10 min. The fluorescence spectra were collected at room temperature using a quartz cuvette on an FL-4600 Fluorescence Spectrophotometer (Hitachi, Japan). The excitation wavelength was 488 nm and the emission wavelength was from 500 nm to 600 nm.

Application to complex biological systems

To assess whether the strategy can be applied in complex biological systems, human dilute serum was adopted as model matrix and recovery tests were performed using the method. Human serum was first diluted 100 times with 20 mM phosphate buffer (5.0 mM Mg^{2+}, pH 7.4). Then the diluted serum was loaded into centrifugal filtration devices (MWCO =50,000 Da, Millipore) and subjected to centrifugation at 6000 rpm for 20 min. For the standard addition experiments, different concentrations of DNA (0.05, 0.5, and 2 nM) were spiked into pretreated human serum and the identical assay procedure as for the aqueous solution was followed.

The serum from volunteer was collected by the first affiliated hospital of Zhengzhou University and informed consent was obtained for the use of human serum. All experiments were performed in compliance with the relevant laws and institutional guidelines and approved by Life-Science Ethics Review Committee of Zhengzhou University.

Characterizations

Transmission electron microscope (TEM) images were performed from JEM-2100 (JEOL, Japan) with a 200 kV accelerating voltage. The FT-IR spectra were performed through a Bruker IFS 66 v/s infrared spectrometer.

Results and discussion

Strategy for DNA detection

The principle of the fluorescence strategy for nucleic acids detection is illustrated in Scheme 1. A molecular beacon (MB) is ingeniously designed, which composes of two DNA domains: (1) a domain complementary to the target DNA, and (2) a domain complementary to the primer. In the absence of the target DNA, the primer and MB is adsorbed on the surface of polydopamine nanotubes via π stacking. Then, with the addtion of the target DNA, target DNA hybridizes with the loop part of MB and unfolds MB to expose the domain complementary to the primer, which subsequently hybridizes with the primer to initiate the polymerization process under the assistance of KF polymerase and dNTPs. The elongated DNA strand thus displaces the target DNA, forming a long dsDNA polymerization products. The released target DNA then hybridizes with an intact MB to initiate the target recycling amplification process. By following this mechanism, a new circular amplification for the target DNA is achieved, forming a large number of dsDNA products. Upon the addition of SG to the reaction solution, a highly enhanced fluorescence signal is generated due to the selective intercalation of SG into dsDNA detached from the polydopamine nanotubes surface, which is directly proportional to the concentrations of the target. However, in the absence of the target DNA, MB maintains the hairpin structure. This is because the hairpin cannot be opened because the stem of MB is 11 bases long while the primer has 8 bases. Thus the amplification processes can not occur, and no dsDNA is formed. Therefore, MB is adsorbed on the surface of polydopamine nanotubes, and the fluorescence of SG is quenched by polydopamine nanotubes, resulting in a low background signal. The signal amplification strategies might provide a fluorometric sensing platform for sensitive and specific detection of DNA.

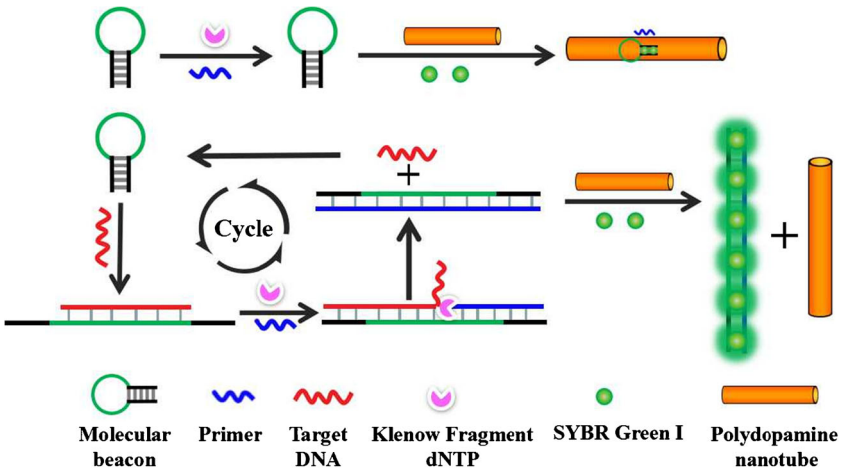

Scheme 1 Schematic of the lable free sensor for sensitive nucleic acids detection by combining cycled strand displacement amplification and the polydopamine nanotube strategy

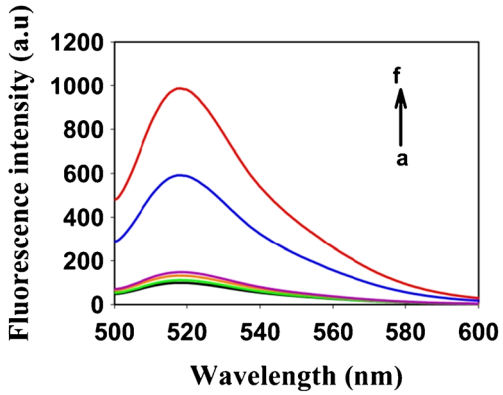

Fig. 1 The fluorescence emission spectra of different sensing systems: (**a**) SYBR Green I; (**b**) MB probe + SYBR Green I + polydopamine nanotubes; (**c**) SYBR Green I + MB probe + Random DNA + Primer 1 + dNTP + Klenow fragment polymerase + polydopamine nanotubes; (**d**) SYBR Green I + MB probe + Primer 1 + dNTP + Klenow Fragment polymerase + polydopamine nanotubes; (**e**) SYBR Green I + MB probe; (**f**) SYBR Green I + MB probe + Target DNA (T1) + Primer 1 + dNTP + Klenow Fragment polymerase + polydopamine nanotubes. (T1, 25 nM; Random DNA, 25 nM; MB, 100 nM; Primer 1, 50 nM; Klenow Fragment polymerase, 30 U/mL; dNTPs, 10 μM; polydopamine nanotubes, 1.2 μg·mL^{-1}; excitation, 488 nm; emission, 518 nm)

Verification of the signal amplification strategy

To confirm the feasibility of this strategy, the fluorescence emission spectra of various condition of the assay are shown in Fig. 1. SG in solution does not exhibit obvious fluorescence emission at 518 nm (curve a). SYBR Green I can bind to MB, the fluorescence intensity of SYBR Green I is significantly enhanced (curve e). In the presence of polydopamine nanotubes and MB, a very weak fluorescence signal of SG was observed (curve b), suggesting that MB and SG were effectively adsorbed on the surface of polydopamine nanotubes With the primer (Primer 1), KF polymerase and dNTP were added into the reaction system, only a slight fluorescence enhancement was observed (curve d), demonstrating that in the absence of the target DNA, no dsDNA was formed and the amplification process did not occur. However, once the target DNA was added to the reaction system, a significant fluorescence enhancement was observed (curve f), indicating that the circular signal amplification for target DNA detection indeed took place. By comparison, with the addtion of random DNA instead of target DNA, a very weak fluorescence signal was observed (curve c), indicating that no dsDNA product was formed. The above results suggested the high selectivity DNA assay can be realized by monitoring the fluorescence signal change.

Fluorescence detection of DNA

The following parameters were first optimized: (a) concentrations of primers and dNTP substrates; (b) reaction time; (c) KF polymerase amount; (d) polydopamine nanotubes concentration. Respective data and Figures are given in the Electronic Supporting Material. The following experimental conditions were found to give best results: (a) A concentrations of primers and dNTP substrates of 50 nM and 10 μM, respectively; (b) a reaction time of 40 min; (c) a KF polymerase amount of 30 U · mL^{-1}; (d) a polydopamine nanotubes concentration of 1.2 μg · mL^{-1}.

Under the above optimal experimental conditions and according to the experimental protocol described in the Experimental Procedures, we investigated the sensitivity of the method by exposing it to a series of target DNA concentrations (0, 0.05, 0.1, 0.5, 1, 5, 10, 25, 50 and 100 nM). As shown in Fig. 2a, the presence of increasing concentration of target DNA from 0.05 to 100 nM leads to gradual increase of the fluorescence intensity. By plotting ΔI_F (ΔI_F=F − F_0, where F and F_0 represents the fluorescence intensity in the presence and absence of target DNA, respectively) vs. the concentration of target DNA, the calibration curve exhibited a good linear relationship (R^2 = 0.993) with a range from 0.05 to 25 nM (Fig. 2b). The limit of detection was estimated to be 20 pM based on three times the standard deviation of the blank tests. The limit of quantification was estimated to be 60 pM with a range from 0.05 to 25 nM. The relative standard deviations of peak fluorescence readings are 3.2%, 2.4%, and

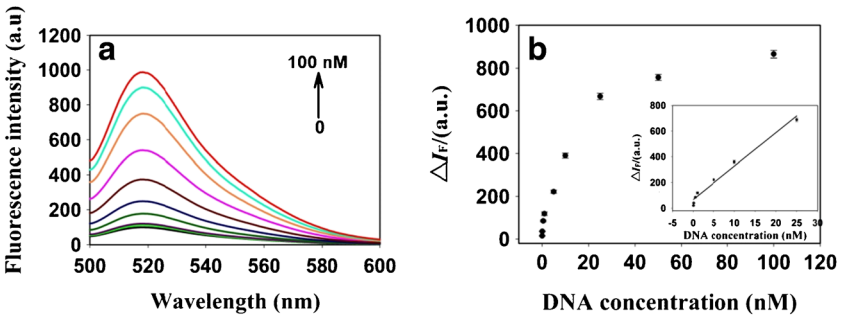

Fig. 2 **a** Fluorescence spectra of the assay system in the presence of increasing amounts of target DNA, the arrow indicates the signal changes at 518 nm with the concentration of DNA increasing (0, 0.05, 0.1, 0.5, 1, 5, 10, 25, 50 and 100 nM). **b** Calibration curve of the assay system for target DNA detection. (MB, 100 nM; Primer 1, 50 nM; Klenow Fragment polymerase, 30 U·mL^{-1}; dNTPs, 10 μM; polydopamine nanotubes, 1.2 μg·mL^{-1}; excitation, 488 nm; emission, 518 nm)

Table 1 Comparison of analytical performance of different methods for DNA detection

Methods	Analytical range	Detection limit	References
Fluorescence	5–500 nM	2 nM	[30]
Fluorescence	0.05–50	40 pM	[31]
Fluorescence	0.05–50	43 pM	[32]
Fluorescence	0.6–3 nM	36 pM	[33]
Chemiluminescence	0.1–3 nM	34 pM	[34]
Fluorescence	0.05–25 nM	20 pM	Our method

2.8% in three repetitive assays of 0.1 nM, 0.5 nM, and 5 nM DNA, respectively, which shows that this proposed method has a good reproducibility. The quenching process is frequently described by the Stern–Volmer equation that can be expressed as: $F_0/F = 1 + K_{SV}[Q]$, where F_0 and F are the fluorescence intensity in the absence and in the presence of quencher, respectively, [Q] indicates the quencher concentration added and Ksv is the Stern–Volmer constant. As shown in Fig. S9, the data are fit by linear analysis, and the Ksv is 1.25×10^{-4} L·mg^{-1}. As shown in Table 1, these analytical parameters are better than previously reported GO-based DNA biosensors [30] or compared favorably with several amplified fluorescence DNA detection methods [31–34]. The experimental results demonstrated that the assay can be used for sensitive DNA detection.

Evaluation of detection selectivity

We evaluated the specificity of this method. The specificity of the DNA assay was studied by testing perfectly matched target DNA (T1), a single base mismatched target DNA (M1), two-base mismatched target DNA (M2), and three-base mismatched target DNA (M3). As shown in Fig. 3, the addition of the mismatched DNA targets only lead to very slight

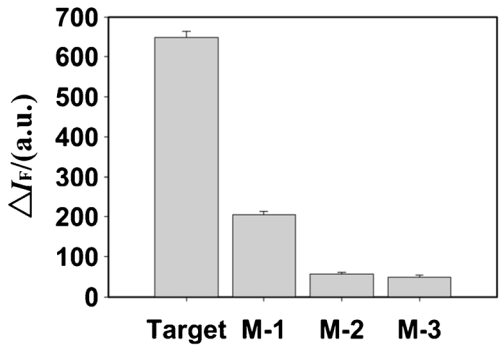

Fig. 3 Comparison of the fluorescence intensity of the biosensing platform at 518 nm in the presence of the target DNA (T1), single-base mismatched target (M1), two-base mismatched target (M2) and three-base mismatched target (M3). (T1, 25 nM; M1, 25 nM; M2, 25 nM; M3, 25 nM; Primer 1, 50 nM; Klenow Fragment polymerase, 30 U·mL^{-1}; dNTPs, 10 μM; polydopamine nanotubes, 1.2 μg·mL^{-1}; excitation, 488 nm; emission, 518 nm)

Table 2 Fluorescence enhancement ratio[a] and tolerance[b] of mismatch DNA M1, M2, and M3 compared to target DNA. [a] Fluoresenceeenhancement ratio of 25 nM mismatch DNA compared to 25 nM target DNA

Mismatch DNA	M1	M2	M3
Response ratio (%)	0.5	0.1	0.1
Tolerance (fold)	10	50	50

[a] Fluoresence enhancement ratio of 25 nM mismatch DNA

[b] Compared to 25 nM target DNA, Fluoresence tolerance of 25 nM mismatch DNA compared to 25 nM target DNA

fluorescence intensity increase. This high specificity arose from the conformational constraint of the stem-loop structure of MB [35], which made it thermodynamically unfavorable for the binding of the mismatched sequences to the loop. These results indicated that the fluorescence strategy has good specificity to distinguish single base mismatched DNA target.

Under optimized condition, the tolerance ratios of M1, M2, and M3 (yielding error lower than 5%) compared to T1 were also tested and listed in Table 2. M2 and M3 showed little interference to the fluorescence at 518 nm, and could exist in 50-fold more than the concentration of M1. The tolerance ratio of M1 was 10-fold.

To assess the application of the sensor in complex biological systems, the analysis of target DNA in human serum was carried out, as detailed in the experimental section. The samples were directly spiked with certain amounts of DNA standard solution and measured by standard addition method. The results are presented in Table 3. High recovery percentage and low standard deviation in the experiments indicate that our strategy for DNA Detection is reliable and has the potential for biological sample application.

Conclusions

In summary, we report a fluorescence strategy for nucleic acids detection by combining strand displacement amplification and the unique features of polydopamine nanotubes and SG. This biosensing strategy exhibits excellent selectivity and sensitivity for DNA assay with low detection limit of 20 pM.

Table 3 Recovery tests for DNA in human serum using the proposed assay

Sample	Added target DNA (nM)	Proposed method mean (nM)[a]	Rcovery(%)
1	0.05	0.049 ± 0.001	98.0%
2	0.50	0.480 ± 0.012	96.0%
3	2.00	1.970 ± 0.021	98.5%

[a] The data were shown as mean (±SD) for three separate measurements, where SD stands for standard deviation

However, it should be noted that DNA was identified by the model in our assay, which still need to improve the sensitivity for DNA detection in real sample. Therefore, the fluorescence DNA assay may become an alternative method for simple and sensitive nucleic acids detection in clinical diagnostics and biochemical researches.

Acknowledgements This work was supported by the National Natural Science Foundation of China (21505122, 21205108), the Startup Research Fund of Zhengzhou University (1511316004), and the Outstanding Young Talent Research Fund of Zhengzhou University (1521316003, 1421316038).

Compliance with ethical standards The authors declare that they have no competing interests.

References

1. Liu JW, Cao ZH, Lu Y (2009) Functional nucleic acid sensors. Chem Rev 109:1948–1998
2. Hang Y, Zhang YL, Xu XM, Jiang JH, Shen GL, Yu RQ (2009) Highly specific and sensitive electrochemical genotyping via gap ligation reaction and surface hybridization detection. J Am Chem Soc 131:2478–2480
3. Zheng J, Jiao AL, Yang RH, Li HM, Li JS, Shi ML, Ma C, Jiang Y, Deng L, Tan WH (2012) Fabricating a reversible and regenerable Raman-active substrate with a biomolecule-controlled DNA nanomachine. J Am Chem Soc 134:19957–19960
4. Zhao JJ, Chu ZD, Jing X, Zhao SL (2015) A fluorescence polarization assay for nucleic acid based on theamplification of hybridization chain reaction and nanoparticles. Sensors Actuators B Chem 209:116–121
5. Ma DL, He HZ, Leung KH, Zhong HJ, Chan DS, Leung CH (2013) Label-free luminescent oligonucleotide-based probes. Chem Soc Rev 42:3427–3440
6. Yin D, Tao YY, Tang L, Li W, Zhang Z, Li JL, Xie GM (2017) Cascade toehold-mediated strand displacement along with non-enzymatic target recycling amplification for the electrochemical determination of the HIV-1 related gene. Microchim Acta 184: 3721–3728
7. Wang XU, Liu WW, Yin BB, Sang YW, Liu ZP, Dai Y, Duan XZ, Zhang G, Ding SJ, Tao ZH (2017) An isothermal strand displacement amplification strategy for nucleic acids using junction forming probes and colorimetric detection. Microchim Acta 184:1603–1610
8. Lee HJ, Li Y, Wark AW, Corn RW (2005) Enzymatically amplified surface plasmon resonance imaging detection of DNA by exonuclease III digestion of DNA microarrays. Anal Chem 77: 5096–5100
9. Shi H, He XX, Yuan Y, Wang KM, Liu D (2010) Nanoparticle-based biocompatible and long-life marker for lysosome labeling and tracking. Anal Chem 82:2213–2220
10. FZ X, Shi H, He XX, Wang KM, He DG, Guo QP, Qing ZH, Yan LA, Ye XS, Li D, Tang JL (2014) Concatemeric dsDNA-templated copper nanoparticles strategy with improved sensitivity and stability based on rolling circle replication and its application in microRNA detection. Anal Chem 86:6976–6982
11. Ge J, Geng X, YH D, Chen JJ, Zhang L, Bai DM, Ji DY, YL H, Li ZH (2017) Highly sensitive fluorescence detection of mercury (II) ions based on WS_2 nanosheets and T7 exonuclease assisted cyclic enzymatic amplification. Sensors Actuators B Chem 249:189–194
12. Wang Y, Li ZH, DH H, Lin CT, Li JH, Lin YH (2010) Aptamer/graphene oxide nanocomplex for in situ molecular probing in living cells. J Am Chem Soc 132:9274–9276
13. Gao C, Guo Z, Liu JH, Huang XJ (2012) The new age of carbon nanotubes: an updated review of functionalized carbon nanotubes in electrochemical sensors. Nano 4:1948–1963
14. Yan LA, Shi H, He XX, Wang KM, Tang JL, Chen M, Ye XS, FZ X, Lei YL (2014) A versatile activatable fluorescence probing platform for cancer cells in vitro and in vivo based on self-assembled aptamer/carbon nanotube ensembles. Anal Chem 86:9271–9277
15. Macak JM, Zlamal M, Krysa J, Schmuki P (2007) Self-organized TiO_2 nanotube layers as highly efficient photocatalysts. Small 3: 300–304
16. Ding W, Wada M, Kameta N, Minamikawa H, Shimizu T, Masuda M (2011) Functionalized organic nanotubes as tubular nonviral gene transfer vector. J Control Release 156:70–75
17. Liu YL, Ai KL, LH L (2014) Polydopamine and its derivative materials: synthesis and promising applications in energy, environmental, and biomedical fields. Chem Rev 114:5057–5115
18. Yu X, Fan HL, Wang L, Jin ZX (2014) Formation of polydopamine nanofibers with the aid of folic acid. Angew Chem Int Ed 53: 12600–12604
19. Lynge ME, van der Westen R, Postma A, Städler B (2011) Polydopamine-a nature-inspired polymer coating for biomedical science. Nano 3:4916–4928
20. Lin LS, Cong ZX, Cao JB, Ke KM, Peng QL, Gao JH, Yang HH, Liu G, Chen XY (2014) Multifunctional Fe_3O_4@polydopamine core-shell nanocomposites for intracellular mRNA detection and imaging-guided photothermal therapy. ACS Nano 8:3876–3883
21. Park J, Brust TF, Lee HJ, Lee SC, Watts VJ, Yeo Y (2014) Polydopamine-based simple and versatile surface modification of polymeric nano drug carriers. ACS Nano 8:3347–3356
22. Fan DQ, Zhu XQ, Zhai QF, Wang EK, Dong SJ (2016) Polydopamine nanotubes as an effective fluorescent quencher for highly sensitive and selective detection of biomolecules assisted with exonuclease III amplification. Anal Chem 88:9158–9165
23. Zhuang J, Fu L, Xu M, Yang H, Chen G, Tang D (2013) Sensitive electrochemical monitoring of nucleic acids coupling DNA nanostructures with hybridization chain reaction. Anal Chim Acta 783: 17–23
24. Xiong E, Zhang X, Liu Y, Zhou J, Yu P, Li X, Chen J (2015) Ultrasensitive electrochemical detection of nucleic acids based on the dual-signaling electrochemical ratiometric method and exonuclease III-assisted target recycling amplification strategy. Anal Chem 87:7291–7296
25. Sun AL, Zhang YF, Wang XN (2015) Sensitive voltammetric determination of DNA via a target-induced strand-displacement reaction using quantum dot-labeled probe DNA. Microchim Acta 182: 1403–1610
26. Murakami T, Sumaoka J, Komiyama M (2009) Sensitive isothermal detection of nucleic-acid sequence by primer generation-rolling circle amplification. Nucleic Acids Res 37:e19
27. Li C, Li Y, Xu X, Wang X, Chen Y, Yang X, Liu F, Li N (2014) Fast and quantitative differentiation of single-base mismatched DNA by initial reaction rate of catalytic hairpin assembly. Biosens Bioelectron 60:57–63
28. Li YB, Li RM, Li Z, Zhang MJ, Ling LS (2017) Fluorometric determination of Simian virus 40 based on strand displacement amplification and triplex DNA using a molecular beacon probe with a guanine-rich fragment of the stem region. Microchim Acta 184:557–562
29. Wang YM, Liu JW, Duan LY, Liu SJ, Jiang JH (2017) Aptamer-based fluorometric determination of ATP by using target-cycling strand displacement amplification and copper nanoclusters. Microchim Acta 184:4183–4188

30. CH L, Li J, Liu JJ, Yang HH, Chen X, Chen GN (2010) Increasing the sensitivity and single-base mismatch selectivity of the molecular beacon using graphene oxide as the "nanoquencher". Chem Eur J 16:4889–4894
31. Liu Y, Liao R, Wang H, Gong H, Chen CY, Chen XM, Cai CQ (2018) Accurate and sensitive fluorescence detection of DNA base on G-quadruplex hairpin DNA. Talanta 176:422–427
32. Wei W, Gao CY, Xiong YX, Zhang YJ, Liu SQ, YP P (2015) A fluorescence method for detection of DNA and DNA methylation based on graphene oxide and restriction endonuclease HpaII. Talanta 131:342–347
33. Zhao CQ, Wu L, Ren JS, XG Q (2011) A label-free fluorescent turn-on enzymatic amplification assay for DNA detection using ligand-responsive G-quadruplex formation. Chem Commun 47: 5461–5463
34. Luo M, Chen X, Zhou GH, Xiang X, Chen L, Ji XH, He ZK (2012) Chemiluminescence biosensors for DNA detection using graphene oxide and a horseradish peroxidase-mimicking DNAzyme. Chem Commun 48:1126–1128
35. Bonnet G, Tyagi S, Libchaber A, Kramer FR (1999) Thermodynamic basis of the enhanced specificity of structured DNA probes. Proc Natl Acad Sci U S A 96:6171–6176